UPPSALA
UNIVERSITET

EVB Simulations of the Reaction Catalyzed by Cytidine Deaminase

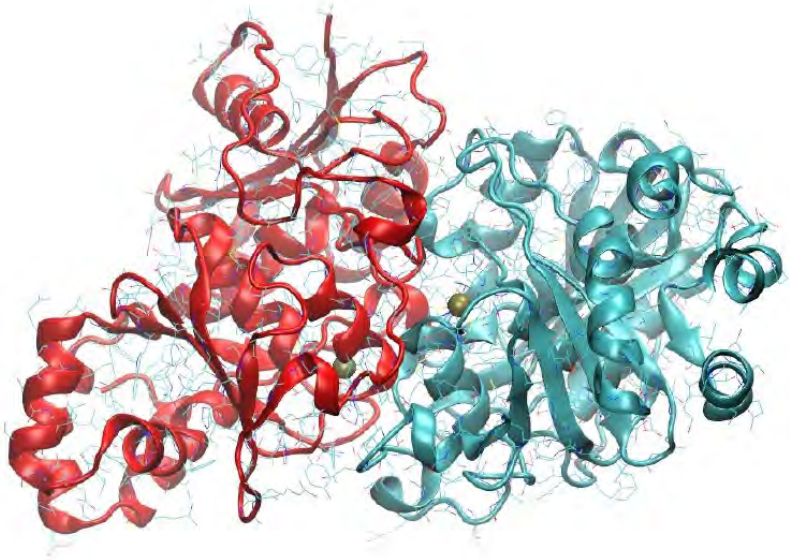

Masoud Kazemi Shalkouhi

Degree project in biology, Master of science (2 years), 2012
Examensarbete i biologi 45 hp till masterexamen, 2012
Biology Education Centre and Department of cell and molecular biology, Uppsala University
Supervisor: Prof. Johan Åqvist
External opponent: Assistant prof. Lynn Kamerlin

CDA	Cytidine deaminase
MD	Molecular dynamics
QM	Quantum mechanics
FEP	Free energy perturbation
EVB	Empirical valence bond
PES	Potential energy surface
KIE	Kinetic isotope effect

Table of Contents

Summary

Cytidine deaminase of *E.coli* is a zinc enzyme that catalysis the deamination of cytidine through a two steps reaction. Its has been shown that the reaction proceed through a tetrahedral intermediate which results in production of uridine and ammonia. Despite, many investigation the exact mechanism of the reaction is to some extent ambiguous. Henceforth, in this project we simulated the enzymatic reaction using empirical valence bond method which is proven to be a very efficient method in addressing these question.

Our simulation shown that the most probable proton pathway before intermediate formation is via Glu104 and the nucleophilic attack on the on C4 of cytidine occur on protonated cytidine. The free energy calculation resulted in 17 Kcal/mol activation energy which is in good agreement with experimental result.

Introduction

Cytidine deaminase

Cytidine deaminase (CDA) from *E.coli* (*EC 3.5.4.5)* is a homo-dimer and each monomer contains one zinc atom. The active site in CDA is located in the interface of two monomers and contains one zinc atom and one glutamic acid residue. The zinc atom is coordinated by two cysteine (Cys 129, 132) and one histidine (His 102) residues. The forth position of zinc coordination is occupied by a water molecule which in turn creates a hydrogen bond with glutamic acid (Glu 104), Figure 1 [16].

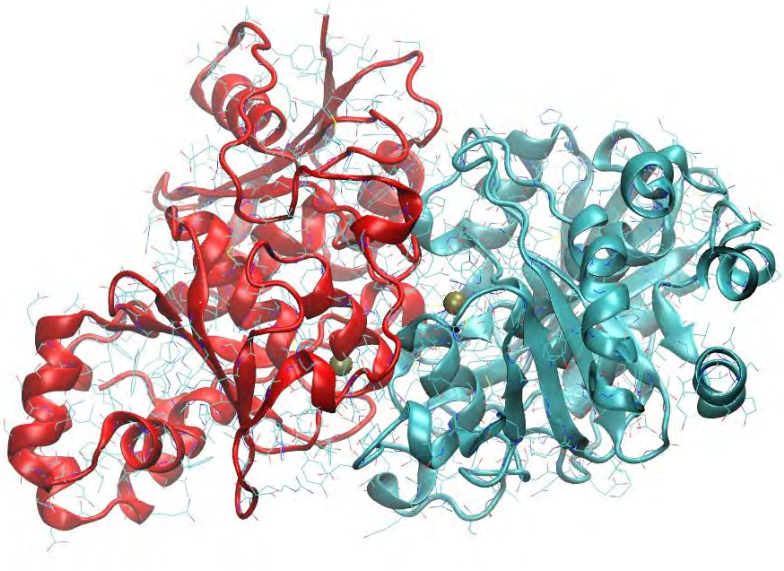

Figure 1: The CDA homo-dimer in ribbon and the snapshot of active site.

The crystal structure of CDA is determined in complex with substrate [17], transition state analog [16] and product [18]. In enzyme-substrate complex, the substrate (cytidine) mainly interacts with a zinc

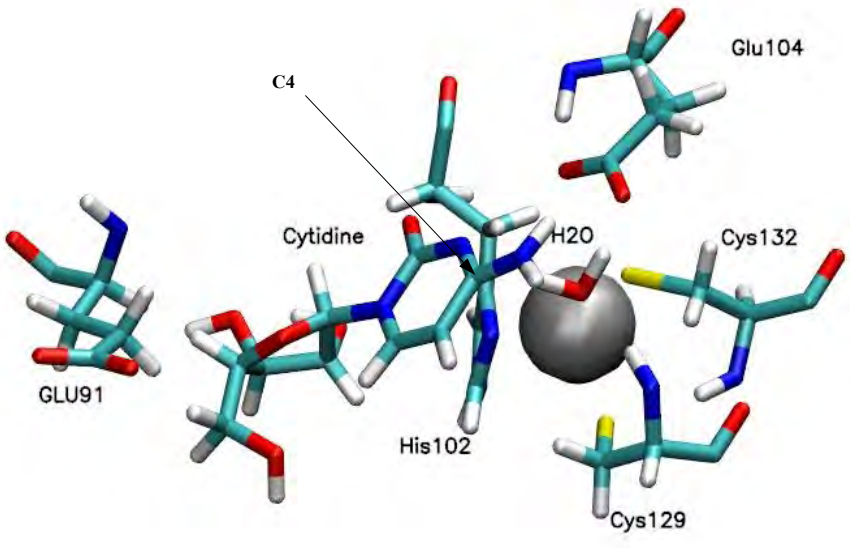

Figure 2: substrate enzyme interactions

bound water and Glu 104 that are in close proximity to reaction center (C4 position on cytidine ring). The substrate also participates in hydrogen binding to Glu 91 via its 3' OH on ribose ring that plays the role of anchor and keeps the cytidine in active site, Figure 2 [16].

CDA catalyzes the deamination of cytidine and kinetics measurements showed that the reaction proceeds as a Michaelis–Menten reaction with k_{cat}=300 s^{-1} and k_{cat}/K_m= 2.8 x 10^{-10} $M^{-1}s^{-1}$. The hydrolytic deamination of cytidine can also happen spontaneously in solution by k_{non} equal to 2.7 x 10^{-10} s^{-1} at 25 ^{o}C. Change in viscosity has no effect on k_{cat}/K_m and k_{cat}; Therefore, it can be concluded that k_{cat}/K_m and k_{cat} are not limited by diffusion rate and product release, respectively, and k_{cat} and K_m are the rate constant of chemical step and dissociation constant, respectively [13].

Transition state analog Zebularine (pyridine-2-one ribofuranoside) is hydrated in active site and inhibits CDA due to its tight binding. Regarding the structure of this component, it has been suggested that the hydrolytic deamination of cytidine occurs through a two steps addition elimination mechanism via a tetrahedral intermediate Figure 3 [2].

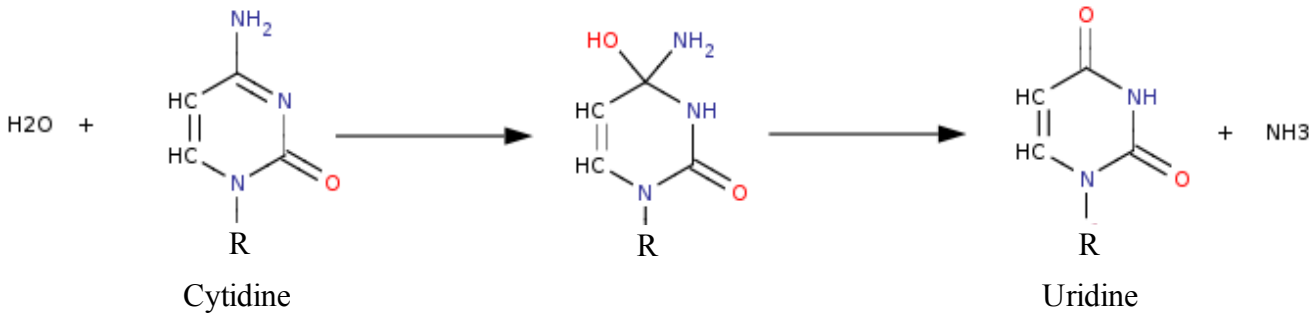

Figure 3: Hydrolytic Deamination of cytidine via the tetrahedral intermediate.

Further evidence regarding the two step addition elimination mechanism of CDA comes from mutation experiments. The mutant E104A shows a dramatic decrease in reaction rate (k_{cat} = 2.6 x10^{-6} s^{-1}) which emphasizes the role of Glu 104. The activity of mutant E104A can be rescued to some extent by formate. The activity rescue is more dominant at higher pH which suggests that the reaction in enzyme is dependent on the deprotonated form of the acid. Considering these evidences, it can be deduced that the reaction occurs via deprotonation of activated water that is coordinated to the forth position of the zinc atom in active site [3]. There is no concrete evidence regarding the proton transfer paths. However, the kinetic isotope effect experiments suggest that the nucleophilic attack of the hydroxyl ion on the 4th carbon position on the ring and production of tetrahedral intermediate is the rate limiting step. Regarding the addition of hydrogen on the N3 of the ring and whether it happens simultaneously with nucleophilic attack or separately no valid statement could be made mainly due to the lack of experimental result and the problem of probing these fast reactions. The solvent deuterium isotope effect has no effect on k_{cat} and shows an inverse effect for k_{cat}/K_m . The proton inventory result for k_{cat}/K_m shows an increase in proton exchange sites which is probably because of water deprotonation. These evidences suggest that water coordinate to the zinc is deprotonated after binding of the substrate and this deprotonation happens before the actual chemistry happens, hence has no effect on the k_{cat} and overall reaction rate. The tetrahedral intermediate undergoes a C-N bond cleavage which results in release of ammonia and production of uridine as the final product [14].

Regarding the spontaneous deamination of cytidine an exact mechanistic picture can not be drawn and despite numerous experiments still is a controversial issue.

The spontaneous deamination of cytidine is a slow reaction and experiments using different catalysts reveal that the hydroxyl ion is by far the most efficient non-enzymatic catalyst, which to some extent suggests a direct nucleophilic attack. The experiment on acid catalysis is not informative mainly because of the competing ring opening reaction, However, the result on deamination of adenosine shows that the low pH also increases the reaction rate. There are different theoretical calculations that propose a mechanistic view of the spontaneous deamination of cytidine which mainly includes the direct attack of one or two water molecule on the ring with different tautomerization states at different pH [5].

Based on these evidences, it could be assumed that the deamination of cytidine proceed through different mechanisms in water and in the enzyme active site. Therefore, in this research we focus our attention mainly on the enzyme catalyzed reaction and we avoid any further discussion concerning the deamination reaction in water considering the ambiguity around the issue and lack of sufficient experiental results.

Molecular dynamics

Molecular dynamics is one of the computational methods that gives a detailed description of interactions of a cluster of particles. In computational biology the main subject of molecular dynamics is the biological molecules e.g. proteins and nucleic acids. At present, considering the progress in computer power it is possible to use all atom models in describing the the biological systems.
In this scenario the interactions of the atoms that create the system are described using the classical mechanics method. Although this approach is not as thorough as the quantum mechanics description, it has been proven to be accurate enough to be used for simulation of biological systems at atomic level in the classical mechanics paradigm.
In molecular dynamics the interaction of atoms is described from classical mechanics perspective which is known as force field. There are a variety of force fields that may be used for different purposes. However, in principle all of them are similar in that they are created in a manner that they can reproduce the physical and chemical properties of the components of interest.
In simplest case the the force field is of the form:

$$U(\vec{r}) = \sum_{bonds} \frac{1}{2} k_b (r_b - r_{b0})^2 + \sum_{angles} \frac{1}{2} k_a (\Theta_a - \Theta_{a0})^2 + \sum_{torsions} \frac{1}{2} k_\Phi (1 + \cos(n_t \Phi_t - \delta_t)) + \sum_{impropers} \frac{1}{2} k_\zeta (\zeta - \zeta_0)^2$$

$$+ \sum_{\substack{nonbonded \\ i>j}} \frac{q_i q_j}{4\pi\epsilon_0 r_{ij}} + \sum_{\substack{nonbonded \\ j>i}} \left(\frac{A_{ij}}{r_{ij}^{12}} - \frac{B_{ij}}{r_{ij}^{6}}\right) \qquad \text{equation 1}$$

According to this equation the potential energy of each system can be calculated by summation of different terms in the equation 1 that correspond to:
Bonding force between to atoms that is described by a harmonic function, the minimum of which corresponds to the the equilibrium distance between two atoms (r_{b0}). The bond constant determines the stiffness of the bond (k_b), Figure 4.

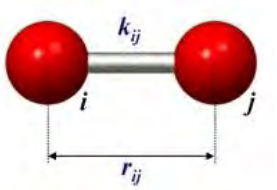

Figure 4: The Bonding parameters

The angle term in the force field function corresponds to the optimum angle between three atoms that are connected by two bonds. This angle is also represented by a harmonic function where its minimum corresponds to the equilibrium angle (Θ_{a0}). The angle constant (k_a) determines the force, Figure 5.

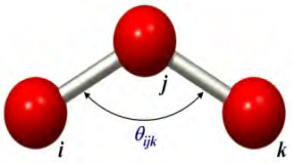

Figure 5: The angle parameters

The torsion term in the force field function corresponds to the angle between four atoms that are connected by three bonds. This angle is represented by a periodic function where its multiplicity (n_t) determines the number of minima in the function and the phase factor is the location of the minima in a 360 ^{0} rotation (δ_t). The improper term in the potential energy function corresponds to the out of plane angle and is represented by a harmonic bond, Figure 6.

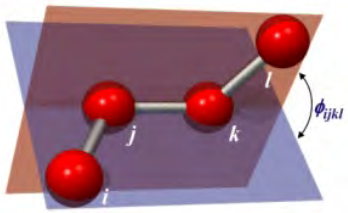

Figure 6: The torsion parameters

The functions mentioned so far are the bonded part of potential function. The second part of potential function corresponds to the non-bonded interactions that are electrostatic interaction which are represented by Coulomb's law. In this term the q is the charge on the particle and the r_{ij} is the distance between two particles, Figure 7.

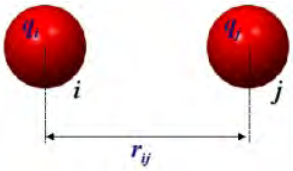

Figure 7: The electrostatic interaction

The last term in potential function is the Lennard-Jones potential, which compared to electrostatic interactions is considered short range. The Lennard-Jones function is composed of two parts. The attraction part works at longer distance and bring two particle into close proximity. The repulsion part works at short distances and when two particles get closer than their van der Waals radius, Figure 8.

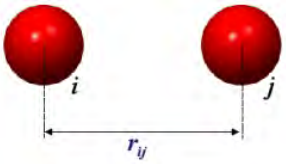

Figure 8: The Van der Waals interaction

Having the potential of each particle based on potential functions, one can calculate the force that act on each particle by differentiation depending on the position of the particle compared to others:

$$\mathbf{F} = -\nabla U_{pot}(r) \qquad \text{equation 2}$$

Once the force acting on each particle has been determined, the position of the particle in a short time step can be calculated based on the Newton's equation of motion:

$$\mathbf{F}_A = m_A \frac{d^2\mathbf{r}_A}{dt^2} \qquad \text{equation 3}$$

The equation 3, as can be seen, is a second order differential equation and the analytical result could only be achieved for simple cases. The biologically interesting problems are composed of thousands of atoms, therefore, solving Newton's equation of motion analytically is not possible. There are many algorithms that address this problem by providing a numerical approach mainly by applying a Taylor expansion. Leap frog is one these algorithms that is considered to be very accurate and simple, equation 4 and 5.

$$\mathbf{v}_A\left(t + \frac{\Delta t}{2}\right) = \mathbf{v}_A\left(t - \frac{\Delta t}{2}\right) + \mathbf{a}_A(t)\,\Delta t + \cdots \qquad \text{equation 4}$$

$$\mathbf{r}_A(t + \Delta t) = \mathbf{r}_A(t) + \mathbf{v}_A\left(t + \frac{\Delta t}{2}\right)\Delta t + \cdots \qquad \text{equation 5}$$

According to this scheme, first the velocity at time $t+\Delta t/2$ is calculated according to equation 4 and using this velocity the position at time $t+\Delta t$ is calculated based on equation 5, hence the name leap frog, since the velocity and position calculations leap over each other at each step of calculation.
In this manner the system gradually reaches a spatial state that corresponds to the lowest energy (as was mentioned, force is the negative gradient of potential energy) and is equilibrium state. However, in the case of a complex potential surface and presence of numerous energy minima the system might not reach a global minimum and be trapped in one of the local minima depending on the starting point of the simulation [10].

Free Energy Perturbation (FEP)

The computational analysis of biological processes is mainly concerned with free energy calculation which is the most general concept in physical chemistry. Many events like protein folding, ligand binding, chemical reaction could be explained and analyzed in term of free energy.
Analytical calculation of free energy using the classical definition of free energy is not possible except for simple systems because an integration over all 3N degrees of freedom for all atoms in a system is needed and in real world problems the number of atoms are in the range of thousands.
On the other hand the free energy difference between two states of a system or related systems can be calculated using Zwanzig's equation, equation 6:

$$\Delta G(A \to B) = G_B - G_A = -k_B T \ln \left\langle \exp\left(-\frac{E_B - E_A}{k_B T}\right)\right\rangle_A \qquad \text{equation 6}$$

In equation 6, T denotes temperature and k_B is Boltzmann's constant. For calculating the free energy

difference according to equation 6, one should simulate the system in the state A and for any configuration the energy is calculated for both states independently. Consequently the free energy could be calculated using Zwanzig's equation by energy difference.
The difference between two states could be a verity parameter. For example, changing atom could be used to mutate the atoms to one another which is widely used in calculation of relative ligand binding free energy calculations and if the two states represent the two states of a reaction the calculated free energy would correspond to the reaction free energy and FEP would be equivalent to the reaction coordinate.
In order to reach convergence and obtain an accurate free energy, it is necessary that the two states be overlapped. In other words, the configuration of state B should be accessible from state A. Fulfilling this criteria implies that the difference between the two states be very small since as it was discussed earlier, molecular dynamics simulation usually results in sampling at near equilibration.
In the biologically relevant problems the above mentioned criteria are not necessarily provided. Therefore, in order to improve the sampling the umbrella-sampling method is widely applied Figure 9.

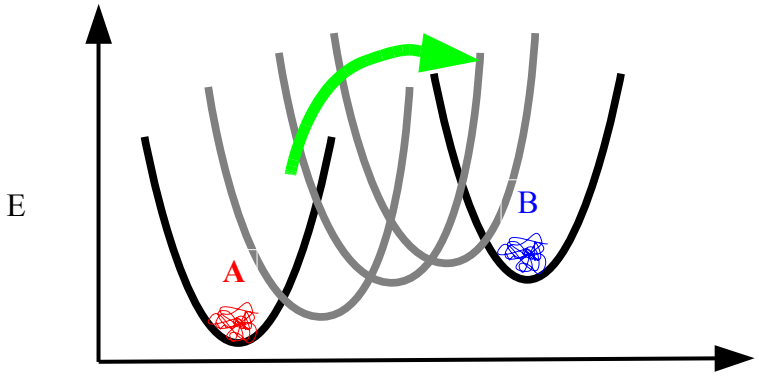

Figure 9: the free energy calculation by Umbrella-sampling

According to the Umbrella-sampling scheme, in process of free energy perturbation the transformation of parameter is broken down to many small steps according to equation 7:

$$E_i = (1-\lambda_i)\, E_A + \lambda_i E_B \qquad \text{equation 7}$$

In this equation the λ is the coupling parameter that result in transformation of the system's parameters in small steps through nonphysical intermediates that connect the two states A and B and λ=0 for state A and λ=1 for state B . Therefore, the free energy difference is a continuous function of the coupling parameter and the free energy is calculated according to equation 8:

$$\Delta G(A \rightarrow B) = G_B - G_A = -k_B T \ln \left\langle \exp\left(-\frac{E_{i+1} - E_i}{k_B T}\right)\right\rangle_A \qquad \text{equation 8}$$

The transformation between two states is performed in both direction (A ►B and B ◄ A). Therefore, for acquiring more accurate result the final free energy is calculated as the mean of forward and reverse transformations, equation 8 [10].

Empirical Valence Bond (EVB)

The EVB is mainly used for simulation and quantitative calculations of chemical reactions, the main underlying idea is that a reaction is represented by valence structures that differ in bond structure and charge distribution, Figure 10.

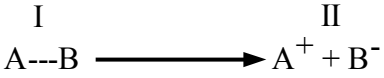

Figure 10: Valence structure of a reaction

The free energy of the reaction is calculated using similar approach as free energy perturbation and umbrella sampling (FEP/US). The different valence structures correspond to the substrate and product and during the simulation the system is transformed between them according to the FEP approach. At each step the energy of two states (E1 and E2) is calculated separately. Figure 11 depicts the evolution of two states potential energy. The two states potential energy would be equal at transition state. The ground state energy is calculated by creating the Hamitonian matrix. The energy of the different states are the diagonal elements of this Hamiltonian matrix and the secular answer of the Hamiltonian is the ground state potential energy of the system, Equation 9. The reaction coordinate is the energy gap between two states (E_2-E_1) at each step.

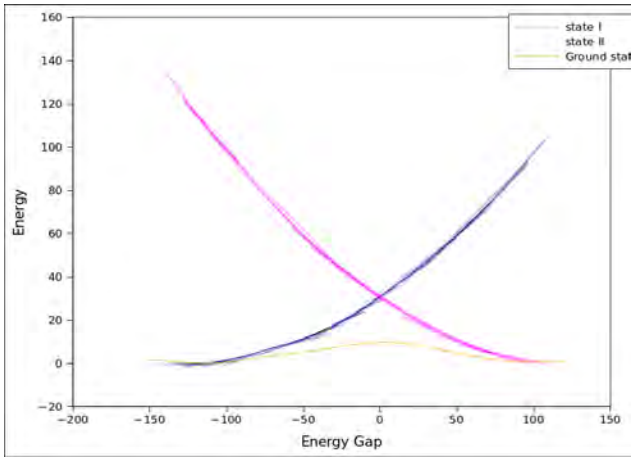

Figure 11: Graph of different states energy and the ground state

One of the most important aspects of EVB is the parametrization of the calculations by the experiments or accurate quantum mechanic calculations. For parametrization, the reaction is first simulated in water without presence of enzyme given that the reaction in enzyme and in water proceeds through same mechanism. Otherwise, the quantum mechanics calculations on the suspected mechanisms has to be performed in water to obtain accurate results. The simulation is parametrized to the available information so that same energy profile is reproduced. The parametrization is performed using the gas shift (α) and the coupling parameter that are the off diagonal elements of Hamiltonian matrix, equation 9.

$$\begin{vmatrix} E1-\alpha & Hij \\ Hij & E2-\alpha \end{vmatrix} = 0 \qquad \text{equation 9}$$

Change in gas shift results in reaction free energy change (the difference in the substrate and product ground state energy) and tuning the off diagonal elements will change the transition state energy (the difference in the energy of substrate and highest point of energy profile), Figure 12. After

parametrization, the reaction is simulated in enzyme and the free energy is calculated using the same parameters that was acquired in the water reaction. Therefore, the difference in activation energy corresponds to the catalytic ability of enzyme which is rooted in the ability of enzyme to stabilize the transition state mainly by electronic interactions [15]. In other words, the difference in activation energy in water and in enzyme can be seen as different solvation ability of transition state in two different environments that is created by water and enzyme active site, Figure 12.

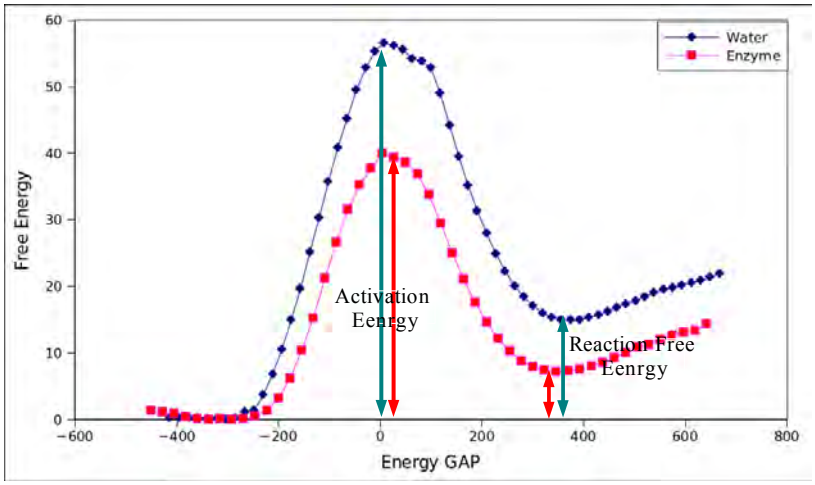

Figure 12: the activation energy and the reaction free energy in water and enzyme.

The calculated result can be compared to the experiments using transition state theory that correlate the activation free energy of a reaction to its velocity and rate constants

$$k = \kappa \frac{k_B T}{h} e^{\frac{-\Delta G^{\ddagger}}{RT}} \qquad \text{equation 10}$$

In equation 10 the k is the reaction rate constant, k_B is Boltzmann's constant, h is plank constant, T is temperature, κ is the probability of reaching to transition state and the number of times that the reactant oscillate over transition state which is usually equal to one in biologically relevant reactions and the $\Delta G^{\S}$ is the activation free energy [15].

The reaction free energy also is correlated to the equilibration constant (K) by equation 11.

$$\Delta G^0 = -RT(\ln K_{eq}) \qquad \text{equation 11}$$

In equation 11, T is temperature, R is gas constant and ΔG^0 is the reaction free energy.

Aim

The aim of this research is creating a model of the enzyme that would be a good representative of the active site and its ability to catalyze the deamination of cytidine. The reaction of deamination is a two step reaction, the first step is the tetrahedral intermediate formation and the second step is the creation of uridine by ammonia as a leaving group. In the degree project we focus on the modeling of the first step. The reaction in active site will be modeled using the empirical valence bond method and further quantum calculation will be performed to determine different protonation pathways that can happen in active site.

Methods

Zinc partial charge calculations

To performe EVB calculations, it is necessary to have accurate force field parameters for all atoms involved in the simulation. Cytidine deaminase is a zinc enzyme and due to the charge transfer ability of this atom, it is problematic to find good parameters. One of these parameters is the partial charge of the zinc atom that could have a major effect on the calculation. Therefore, its accurate calculation is of great importance. The partial charge on the zinc was calculated using ChelpG methods [1] and CPCM water continuum solvent [4] by Gaussian 09 QM package [6]. For this population analysis calculation the B3LYP Density functional theory with 6-31G* basis set was used. Figure 13 depicts the fragment of active site that was used for this calculation and all free ends were caped by methyl groups.

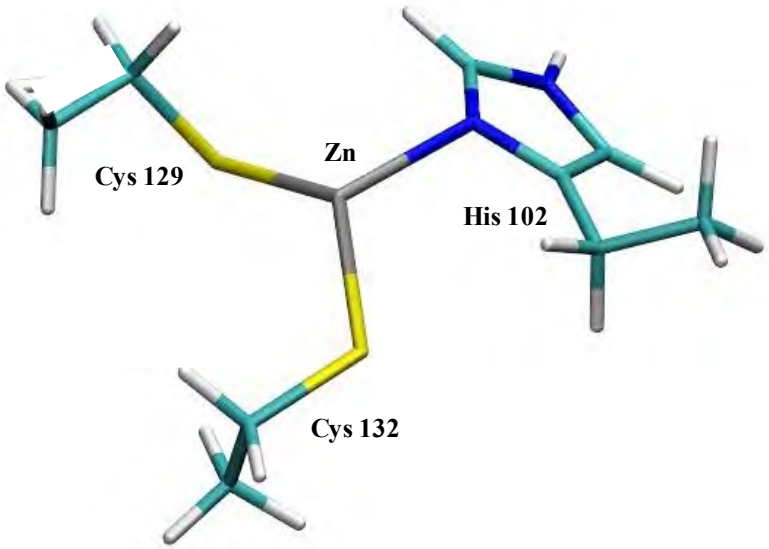

Figure 13: The active site fragment used for partial charge calculation

The atomic radii for these calculation was as follow: Zn 1.39, N 1.55, C 1.70, H 1.09, S 1.80 , O 1.52 Å. The total charge of the system was set to zero and considering the presence of two deprotonated cysteine residues the oxidation state of zinc would be +2.

Potential energy surface calculations (PES):

To investigate the underlying mechanism of intermediate formation by nucleophilic attack and the possible transition state structure the PES of reaction was calculated. The intermediate and the acetic acid (as a model for Glu 104) was used as starting point for PES calculations, Figure 14.
At each point of potential energy surface the distance of N3—H and C4—OH bonds of the intermediate was kept constant and the rest of cluster was optimized using B3LYP/6-31+G* and SMD continuum solvent, due to the better performance of SMD solvent model in calculation of free energy for charged species [12]. For each step the mentioned distances were increased by 0.1 Å. At each step following the structure optimization the energy of cluster was calculated using B3LYP/6-311+G** which is a bigger basis set in order to increase the accuracy of energy calculation. The resulting energy was compared to the energy of intermediate and acetic acid at infinite separation.

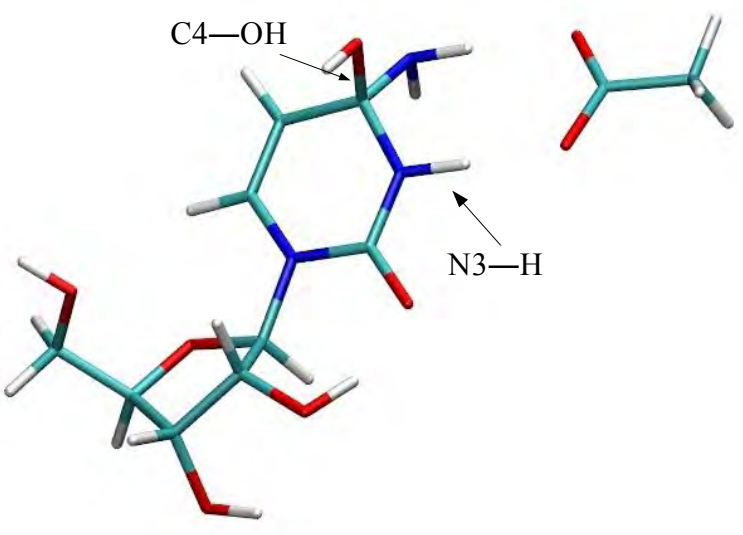

Figure 14: The starting structure for PES calculations

Calculation of reaction free energy in water as the reference point

For EVB calculations the reference point energy is needed for parametrization of the water reaction. Since the mechanism of the reaction that occurs in water is different from that in the cytidine deaminase active site, the reaction free energy of the suspected mechanism was calculated using quantum mechanics calculations as a reference point. For reference point calculation, the intermediate formation reaction was broken down into the following steps:

Step1:

Water deprotonation which can proceed either by transfer of hydrogen to the Glu 104 and further transport of hydrogen to the cytidine:

$$HOH + Glu\text{-}COO^- + Cytidine \longrightarrow OH^- + Glu\text{-}COOH + Cytidine$$

$$OH^- + Glu\text{-}COOH + Cytidine \longrightarrow OH^- + Glu\text{-}COO^- + Cytidine\text{-}H^+$$

Alternatively, the hydrogen could be directly transfer to the cytidine following the deprotonation of water:

$$HOH + Glu\text{-}COO^- + Cytidine \longrightarrow OH^- + Glu\text{-}COO^- + Cytidine\text{-}H^+$$

For calculation of the reaction free energy of the proton transfer reaction as reference point the difference between proton donor and accepter point was used according to equation 12 [9].

$$\Delta G^0_{depro} = 2.3\ RT\ (pKa_{donor} - pKa_{acceptor}) \qquad \text{equation 12}$$

The pKa value that was used for these calculations are as follow, 15.75 for H_2O, 5.5 for Glu and 4.5 for cytidine.

Step 2:

Following the deprotonation the nucleophilic attack would occur that results in tetrahedral intermediate formation. Calculating the reaction free energy of the nucleophilic attack was performed using a

thermodynamic cycle, Figure 15 [7].

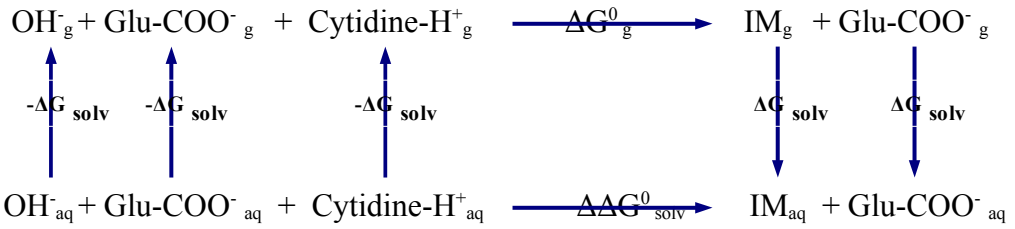

Figure 15: Thermodynamic cycle used for reaction free energy calculation

The reaction free energy in water (ΔG^0_{aq}) can be calculated according to the equation 13 [7].

$$\Delta G^0_{aq} = \Delta G^0_{g} + \Delta\Delta G^0_{solv} \qquad \text{equation 13}$$

In equation 13, ΔG^0_{g} is the reaction free energy in the gas phase that can be calculated by equation 14 [7].

$$\Delta G^0_{g} = G_{product} - G_{reactant} \qquad \text{equation 14}$$

For ΔG^0_{g} calculation the structure of all species in the reaction were optimized using B3LYP/6-31+G* at continuum solvent SMD and the potential energy of the optimized structure was calculated in gas phase using B3LYP/6-311+G**. For thermal and zero point corrections frequency analysis was performed using B3LYP/6-311+G**. The $\Delta\Delta G^0_{solv}$ in equation 13 can be calculated by equation 15 [7]:

$$\Delta\Delta G^0_{solv} = \Delta G^0_{solv\text{-}product} - \Delta G^0_{solv\text{-}reactant} \qquad \text{equation 15}$$

Solvation energy is the energy needed for moving a molecule from gas phase to the solution. Since the reaction contains species like OH^- for which the solvation energy calculation is error prone, the bench mark value for solvation energy was used expect for cytidine, protonated cytidine and intermediate species which were calculate using B3LYP/6-311+G** and SMD continuum solvent that is parametrized for organic components. The solvation energy used for different species was taken from the Josefredo et al work [8] that suggests bench mark value for common species in biochemistry with standard state correction in order to avoid the deficiency in solvation energy calculation of charged molecules present in the calculation. These are -28.0 Kcal/mol for cytidine, -77.3 Kcal/mol for CH_3COO^-, -6.7 Kcal/mol for CH_3COOH, -6.32 Kcal/mol for H_2O, -16.67 Kcal/mol for intermediate, -105.0 Kcal/mol for OH^- and -71.39 Kcal/mol for protonated cytidine.

Zinc parameter and enzyme equilibration

For doing any calculation using molecular dynamics accurate parameter for zinc ion is needed. The partial charge on zinc atom was calculated using quantum mechanics methods. In the cytidine deaminase crystal the zinc shows a tetrahedral coordination. However, the single charge point approach that is conventional in molecular dynamics would not keep such configuration. To avoid such a problem the charge on zinc atom was transferred to four dummy interaction points around the central zinc. These four dummy charges have no van der Waals interactions and only hold the charge on zinc in a tetrahedral configuration. The central atom in this tetrahedral structure have van der Waals interactions, Figure 16.

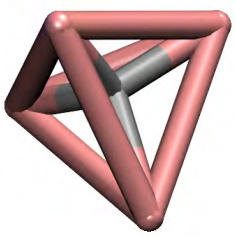

Figure 16: zinc tetrahedral structure.

The zinc parameter is directly determined by its intermediate coordination. Therefore, during the parametrization of zinc atom different parameters were changed until the model produced a structure similar to that in the crystal of cytidine deaminase. During this process, after assigning different parameters a relaxation MD procedure was applied in order to make sure that the chosen parameters are able to reproduce the crystal structure conformation. The molecular dynamics was performed using Q package [11] with spherical boundary condition.

In this simulation the region of interest is placed inside a sphere and the rest of the system which does not have great effect on the calculation remain outside and constraints keep it in place. The radius of simulation sphere was 14 Å and the simulation was performed on the dimer of the enzyme. Since two active sites are at 15 Å distance from each other, one of the active sites would be near the boundary which makes the simulation unstable. Therefore, one of the active sites was deactivated and all of the charged groups were replaced with neutral counterparts. In the remaining active site the residues Glu 104, Cys 129, Cys 132 and Glu 91 were set to their ionized state since they are assumed to play an important role in the catalysis. The simulation was performed with TIP3P explicit water and the 10 Å cut off was used for long range interactions.

The relaxation was performed in the conventional way that includes five steps of simulation with temperatures of 1K, 50K, 150K and 298.5K. During the first four steps tight bath coupling were used for fine tuning of temperature. In the last stage the simulation temperature was set to 298.5K with a loose bath coupling. During the reaction, there are three different species that occupy the forth coordinate of zinc. Therefore, the above mentioned procedure was tested for each set of parameters for all different coordinations in order to make sure that the selected parameters produce stable structure similar to the crystal structure.

EVB procedure

During EVB free energy calculations, the reaction is represented by different valence structures. In order to obtain reliable results, it is necessary that different scenarios are examined so that an accurate conclusion can be drawn regrading the reaction path.
In this project the EVB calculation was performed for two different scenarios that were assumed to be important. In both scenarios the nucleophilic attack occurs after water deprotonation and cytidine protonation. However, the proton transfer pathway differs in two different ways.
In first case the proton is transfered from water to Glu104 which subsequently is passed to cytidine. This pathway was modeled in three stages. The first simulation is represented by two valence structures , Figure 17:

$$HOH + Glu\text{-}COO^- \longrightarrow OH^- + Glu\text{-}COOH$$

State I State II

Figure 17: the valence structures of Glu104 protonation

This reaction was simulated in water and the result was parametrized to proton transfer reaction according to equation 12. Subsequently, the same reaction was simulated in active site and the free energy calculation was performed using the parameters of water reaction. The simulation was performed using Q package at 298.5 K temperature and spherical boundary condition with condition similar to relaxation step. The starting structure was the output of relaxation procedure [11]. During EVB run for the atoms that were involved in bond breaking and forming soft potential was used and all bond parameters were described by Morse potential. The transformation between the two valence structures was performed in 51 windows which gradually shift from state I toward state II. The detailed description of two states is available in appendix A.
The second stage of this reaction is represented by Figure 18:

$$\underset{\text{State I}}{\text{Glu-COOH} + \text{Cytidine}} \longrightarrow \underset{\text{State II}}{\text{Glu-COO}^- + \text{Cytidine-H}^+}$$

Figure 18: protonation of cytidine via Glu104

The second stage is the protonation of cytidine by protonated Glu104. This reaction was also performed both in water and in the enzyme and parametrization was performed using equation 12. The simulation details are as before and the detailed description of two states is available in appendix B.
The third stage of this pathway is the nucleophilic attack of hydroxyl ion to the protonated cytidine. This reaction was simulated in water and the water reaction was parametrized to the reaction free energy and suggested transition state resulted from quantum mechanics calculations. The acquired parameters used for free energy calculation of enzyme catalyzed reaction. This step is represented by Figure 19.

$$\underset{\text{State I}}{\text{OH}^- + \text{Glu-COO}^- + \text{Cytidine-H}^+} \longrightarrow \underset{\text{State II}}{\text{IM} + \text{Glu-COO}^-}$$

Figure 19: nucleophilic attack on the protonated cytidine

Since the quantum mechanics calculations was performed in presence of acid, in EVB water reaction the acid was also included in order to allow the QM result to be used for parametrization. The description of two state is available in appendix C.
The second scenario that was simulated using EVB approach is the direct protonation of cytidine by water prior to nucleophilic attack. This reaction is represented by Figure 20:

$$\underset{\text{State I}}{\text{HOH} + \text{Cytidine}} \longrightarrow \underset{\text{State II}}{\text{OH}^- + \text{Cytidine-H}^+}$$

Figure 20: Direct protonation of cytidine by water

The water reaction was parametrized using equation 12 and the description of two states is available in appendix C. For this scenario the nucleophilic attack of hydroxyl ion is simulate as mentioned before.

Results

Zinc parameters

The zinc ion is capable of charge transfer. Therefore, in order to obtain an accurate description of the charge distribution, a population analysis was performed. The results suggest that the partial charge on the zinc ion is +1. According to this result the +1 charge was assigned to zinc and was distributed on the four charge dummies around the zinc atom with tetrahedral coordination. Further tuning of partial charge and van der Waals parameters of the system was performed during relaxation process until a stable structure was obtained which is similar to the crystal structure. The best results that were obtained are depicted in Table 1 and Figure 21.

[Zn]	name	Type	Partial Charge				
1	ZN1	ZNN	0.0				
2	DZ2	DZZ	0.25				
3	DZ3	DZZ	0.25				
4	DZ4	DZZ	0.25				
5	DZ5	DZZ	0.25				
Zn vdW parameters							
ZNN	50.00	50.00	3.36	15.54	2.38	53.38	
DZZ	0.00	0.00	0.00	0.00	0.00	3.00	
Zn bond parameters							
ZNN	DZZ	1280.0	0.900				
DZZ	DZZ	1280.0	1.470				
Zn angle parameters							
DZZ	ZNN	DZZ	110.000	109.500	0.000	0.000	
DZZ	DZZ	DZZ	110.000	60.000	0.000	0.000	
DZZ	DZZ	ZNN	110.000	35.250	0.000	0.000	
Zn torsion parameters							
ZNN	DZZ	DZZ	DZZ	0.000	2.000	35.300	1
DZZ	ZNN	DZZ	DZZ	0.000	2.000	120.000	1
DZZ	DZZ	DZZ	DZZ	0.000	2.000	70.500	1

Table 1: The optimized zinc parameters

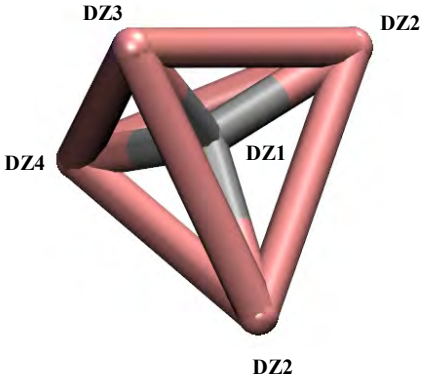

Figure 21: The tetrahedral structure of zinc

The zinc atom in the active site is coordinated to His 102, Cys 129 and Cys 132. For these amino acids the standard Oplsaa parameters were used except for partial charges that were as depicted in Figure 22:

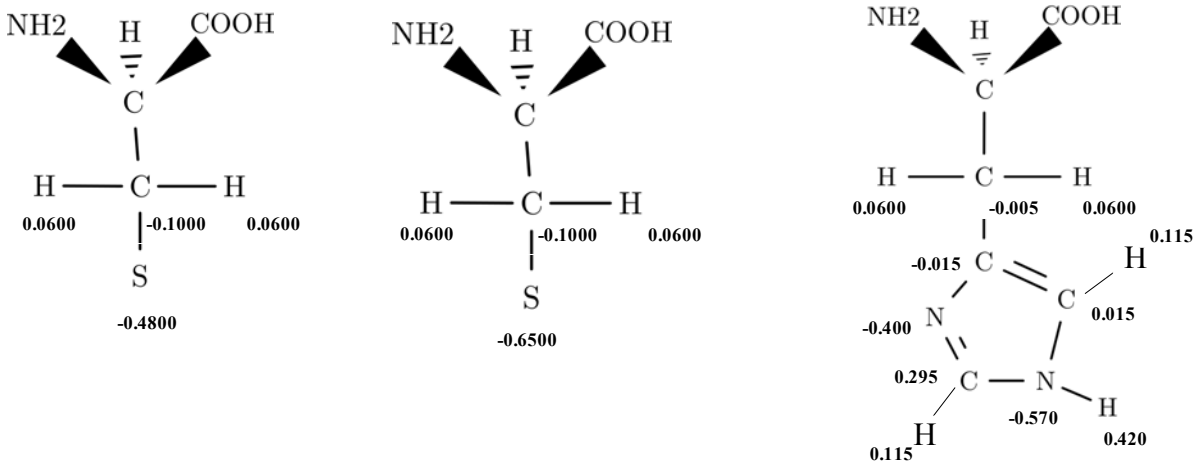

Cys132 Cys129 His102

Figure 22: Partial charge distribution on residues Cys132, Cys129 and His102

Using this set of parameters we were able to reach a fairly stable structure for the zinc atom that is coordinated to H_2O and OH^- on the forth coordinate. During 20 picosecond of last stage of relaxation, the average distances between the ND1 nitrogen atom of His102, sulfur atoms of Cys 129 and Cys132 from zinc atom in the model are 2.18 Å (0.07 standard deviation), 2.26 Å (0.07 standard deviation) and 2.28 Å (0.07 standard deviation) respectively and the corresponding distances in the crystal structure are 2.38 Å, 2.39 Å and 2.18 Å respectively. On the other hand, when the intermediate is coordinated to the zinc atom the structure become slightly unstable and 5 Kcal/mol distance restraints between zinc atom and Glu 104 COO^- group was used in order to make the structure stable during EVB calculations. The 5 Kcal/mol distance restraint resulted in on average 0.39 Kcal/mol energy on the system with 0.35 standard deviation at last stage of equilibration of system, Figure 23.

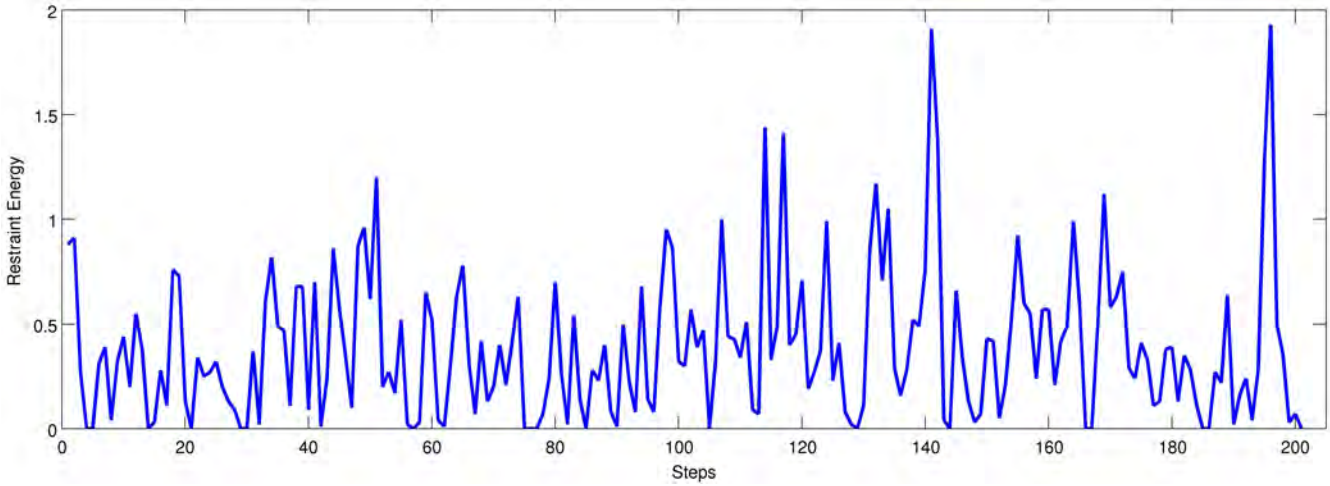

Figure 23: The energy of distance restraint that is exerted on the system during last stage of equilibration.

Potential Energy Surface:

The calculated potential energy surface in this case could not be used for calculation of activation energy mainly due to the fact that the present charged groups, e.g. OH^-, COO^- and protonated cytidine give rise to the solvation energy error. However, this calculation could provide an overall view of the reaction mechanism. In this calculation two degrees of freedom in the reaction coordinate were scanned, which compare the simultaneous addition of H to N3 and OH to C4 to stepwise addition of H to N3 and OH to the C4. The result clearly suggests that the reaction happens via a stepwise process and the nucleophilic attack of OH to C4 happens after protonation of cytidine, Figure 24.

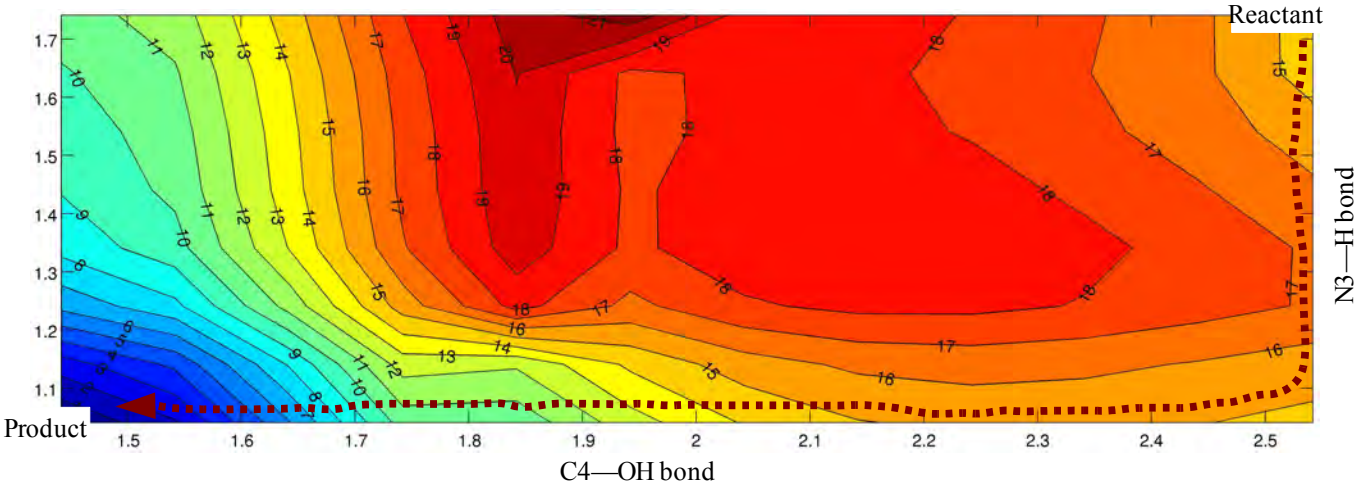

Figure 24: potential energy surface of nucleophilic attack.

As can be seen from Figure 24, for the reaction to happen via a concerted pathway, the reactants have to pass through a higher transition state. Moreover, Figure 24 shows that the energy level of reactant is around 15Kcal higher than product which clearly is in contrast to the reaction free energy calculation of the reaction at infinite separation. This result is mainly due to two factors. First it was not possible to track the reaction to the reactants state with an appropriate separation because of high reactivity of hydroxyl ion and its attack to the amine group on C4. Second, presence of charged species like hydroxyl ion and carboxylic acid at reactant state results in 10 Kcal/mol and 3 Kcal/mol underestimation of solvation energy for OH^- and CH_3COO^- respectively that reveals itself in PES as a higher level energy of reactants.
Despite all systematic errors, this calculation can be used as a comparison between three possibilities of protonation of cytidine in the presence of glutamic acid. The most favorable transition state according to this calculation is the nucleophilic attack of the hydroxyl ion on the protonated cytidine. The corresponding transition state was further analyzed using frequency analysis, which resulted in the presence of one imaginary vibrational frequency that further supports the hypothesis that the selected structure is the true transition state, Figure 25.

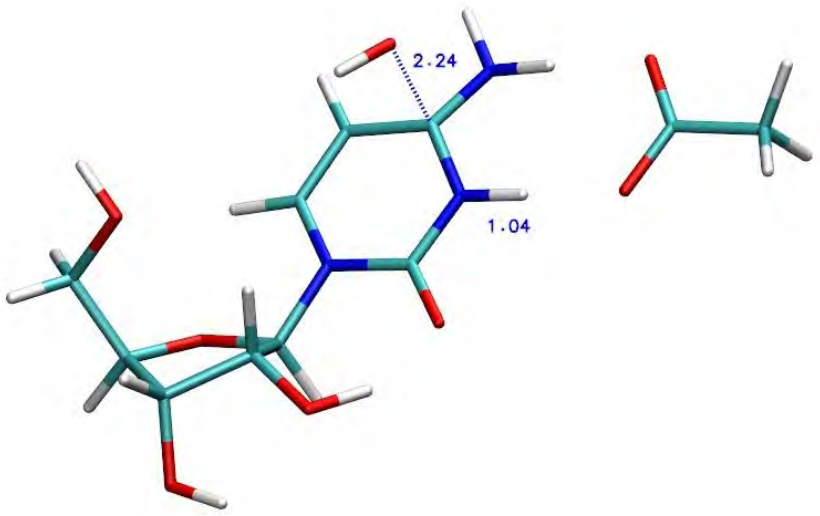

Figure 25: The proposed transition state according to the PES calculating

For activation energy calculation, the relative energy difference of transition state was first calculated against the product (intermediate) in order to avoid the solvation energy error in the reactant state. Afterwards, considering the reaction free energy of the reactant and product the activation energy was calculated.

EVB calculations

Two scenarios for intermediate formation was analyzed by EVB calculation. In the fist case the proton transfer to Glu104 (A) and subsequent protonation of cytidine (B) followed by nucleophilic attack of OH on the C4 (C) was modeled which resulted in the energy profile shown in Figure 26.
The ΔG^0_{depro} for deprotonation of water and proton transfer to Glu 104 in enzyme is 0.55. ΔG^0 for proton transfer from Glu 104 to cytidne is equal to -10.40 and finally the ΔG^0 for OH nucleophilic attack is 11.65. The activation free energy ($\Delta G^{\S}$)for this step in enzyme is equal to 17.22.
The simulation of direct protonation of cytidine by water dramatically destabilized the active site structure and therefore no free energy could be calculated.

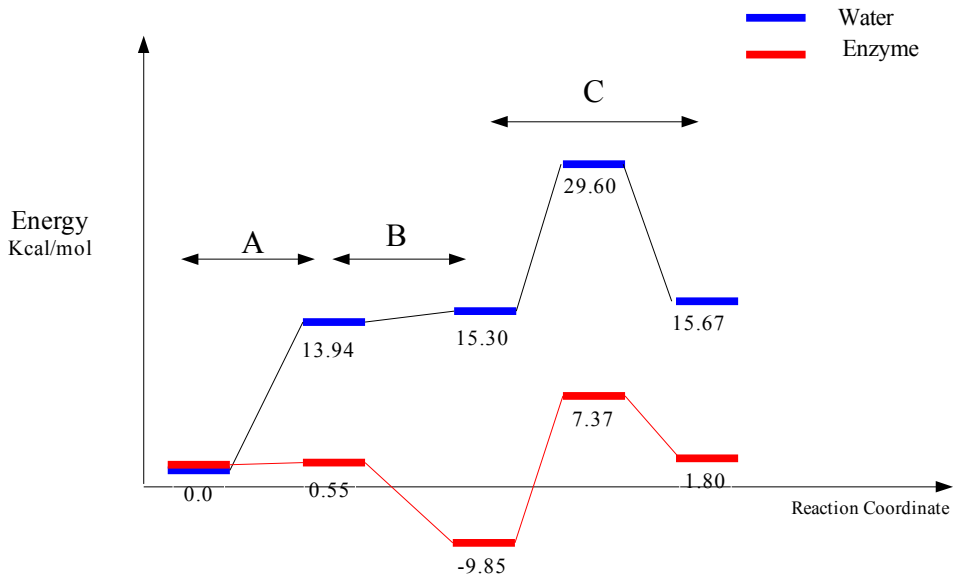

Figure 26: Intermediate formation energy profile in water and in enzyme.

Discussion

In this project we tried to model the reaction catalyzed by cytidine deaminase. This enzyme uses zinc as cofactor, hence at first step we created a model that would be representative of the active site using the dummy charge approach. It has been shown that despite the relative stability of the system, upon change in the coordination of the zinc metal the active site suffer from some degrees of instability which can be explained by the charge transfer ability of the the zinc. In these simulations a static model used for charge distribution on zinc and its immediate coordinated atoms. However, it seems that a dynamic model and changing the partial charge distribution at different valence structures according to the valence configuration could be better representative of the charge distribution in the active site considering the nature of zinc metal. Moreover, using a dummy model for keeping the configuration of zinc metal introduces some artifacts. In this model the dummy charges are kept in place by bond terms which in turn result in a vibration of charges in a time scale that could be sensed by system. This situation is in contrast to one of the main assumptions of molecular dynamics that the electron movements are extremely fast that they adopt to the nucleus movements in a way that their motions are not sensed in the time scale of the molecular dynamics. This artificial charge vibration results in constructive frequency motions that results in collapse of the system. Despite all these drawbacks we were able to stabilize the system mainly without using any restraints except for the nucleophilic attack stage that 5 Kcal/mol restraints were used which makes a very small contribution in final free energy.
Having this model we examined different scenarios by which this reaction might occur. The viscosity experiments prove that the K_{cat} is not affected by diffusion. Therefore, it corresponds to the rate limiting step of chemical reaction. The observed activation energy of the enzyme is around 14 Kcal/mol [13] which in comparison to our calculated value shows a 3 Kcal/mol deviation. The QM calculations resulted in 14 Kcal/mol activation free energy in water for OH nucleophilic attack. However, because the protonation reactions are extremely unfavorable this reaction do not happen in water. It can be noticed that the main source of catalysis is coming from carboxylic acid and the main role of Zn is probably the activation of water. The 3 Kcal deviation of observed value might be due to the lack of proper convergence and more gradual transformation and longer simulations might improve the result.

In this project we addressed several questions that could not be answered experimentally. According to the transition state analog experiment, it has been proven that this reaction proceed through a tetrahedral intermediate and kinetics isotope effects suggested that the rate limiting step is the tetrahedral formation [6,7]. However, no information regarding the mechanism of the proton transfer is available. The potential energy surface clearly suggests that the OH nucleophilic attack happens on protonated cytidine. Moreover, considering the fact that the EVB simulation of the direct protonation of the cytidine by water results in the active site instability, one can conclude that this mechanism is not probable due to spatial constraints.

Appendix

A: Glu104 protonation

```
[atoms]
1  1528
2  1529
3  1530
4  1531
5  1532
6  1533
7  1534
8  1535
9  1536
10  1537
11  1538
12  1539
13  1540
14  1541
15  1542
16  4446
17  4447
18  4448

[change_charges]
1  -0.5000   -0.5000
2  0.3000    0.3000
3  0.1400    0.1400
4  0.0600    0.0600
5  -0.1200   -0.1200
6  0.0600    0.0600
7  0.0600    0.0600
8  -0.2200   -0.1200
9  0.0600    0.0600
10  0.0600   0.0600
11  0.7000   0.5200
12  -0.8000  -0.5300
13  -0.8000  -0.4400
14  0.5000   0.5000
15  -0.5000  -0.5000
16  -0.8340  -1.2000
17  0.4170   0.4500
18  0.4170   0.2000

[atom_types]
C          1802.24   34.18     0.00     0.00     1274.38   24.17    12.01
OHO1   856.00    0.00     70.00     1.581    856.00    23.01    16.00
CT        944.52    22.03     0.00     0.00     667.88    15.58    12.01
N         971.75    28.31     0.00     0.00     687.13    20.02    14.01
OHH2      0.00      0.00      0.00     0.00     0.00      0.00     1.01
OW       762.89    24.39     70.00     1.581    539.45    17.25    16.00
O         616.44    23.77     0.00     0.00     435.89    16.81    16.00
HC        84.57     5.41      0.00     0.00     59.80     3.83     1.01
O2        616.44    23.77     70.00     1.581    435.89    16.81    16.00
HO          0.00      0.00      6.50     1.581    0.00      0.00     1.01
HC1       84.57     5.41      0.00     0.00     59.80     3.83     1.01
C2        1802.24   34.18     0.00     0.00     1274.38   24.17    12.01
ODE       601.15    22.27     70.00     1.581    425.08    15.74    16.00
H           0.00      0.00      0.00     0.00     0.00      0.00     1.01
HW          0.00      0.00      6.50     1.581    0.00      0.00     1.01

[change_atoms]
1  N  N
2  H  H
3  CT  CT
4  HC  HC
5  CT  CT
6  HC1  HC
7  HC1  HC
8  CT  CT
9  HC  HC
10  HC  HC
11  C2  C2
```

```
12  O2  ODE
13  O2  O
14  C  C
15  O  O
16  OW  OHO1
17  HW  HO
18  HW  OHH2

[soft_pairs]
16   17
12   17

[bond_types]
1 142.500  2.00  1.229
2 138.250  2.00  0.945
3 138.250  2.00  0.957
4 112.500  2.00  1.364
5 164.000  2.00  1.250

[change_bonds]
1538  1539  5    4
1538  1540  5    1
4446  4447  3    0
1539  4447  0    2

[angle_types]
1 200.000  104.520
2  70.000  113.000
3 140.000  117.000
4 160.000  120.400

[change_angles]
1535  1538  1540    3    4
4447  4446  4448    1    0
1538  1539  4447    0    2

[torsion_types]
1   1.500   -1.000    0.000
2   0.000    1.000    0.000
3   2.450    2.000  180.000
4   0.000    2.000  180.000

[change_torsions]
1536  1535  1538  1540    2    0
1537  1535  1538  1540    2    0
1536  1535  1538  1540    0    4
1537  1535  1538  1540    0    4
1535  1538  1539  4447    0    1
1535  1538  1539  4447    0    3
1540  1538  1539  4447    0    3

[off_diagonals]
1    2    12    16    1.00  0.50
```

B: cytidine protonation via Glu104

```
[atoms]
1  1528
2  1529
3  1530
4  1531
5  1532
6  1533
7  1534
8  1535
9  1536
10  1537
11  1538
12  1539
13  1540
14  1541
15  1542
16  1543
```

17 4417
18 4418
19 4419
20 4420
21 4421
22 4422
23 4423
24 4424
25 4425
26 4426
27 4427
28 4428
29 4429
30 4430
31 4431
32 4432
33 4433
34 4434
35 4435
36 4436
37 4437
38 4438
39 4439
40 4440
41 4441
42 4442
43 4443
44 4444
45 4445
46 4446

[change_charges]
1 -0.5000 -0.5000
2 0.3000 0.3000
3 0.1400 0.1400
4 0.0600 0.0600
5 -0.1200 -0.1200
6 0.0600 0.0600
7 0.0600 0.0600
8 -0.1200 -0.2200
9 0.0600 0.0600
10 0.0600 0.0600
11 0.5200 0.7000
12 -0.5300 -0.8000
13 -0.4400 -0.8000
14 0.4500 0.4800
15 0.5000 0.5000
16 -0.5000 -0.5000
17 -0.6830 -0.6830
18 0.1450 0.1450
19 0.1700 0.1700
20 -0.4225 -0.4225
21 0.2050 0.2050
22 -0.7000 -0.7000
23 0.2050 0.2050
24 -0.7000 -0.7000
25 0.4725 0.5325
26 -0.5600 -0.6200
27 0.5500 0.6500
28 -0.4800 -0.3000
29 -0.5400 -0.7400
30 0.4600 0.6600
31 -0.7900 -0.8100
32 -0.0600 -0.0075
33 0.1000 0.1525
34 0.4180 0.4180
35 0.0600 0.0600
36 0.0600 0.0600
37 0.0300 0.0300
38 0.0600 0.0600
39 0.4350 0.4350
40 0.0600 0.0600

41 0.4350 0.4350
42 0.1300 0.1600
43 0.3700 0.4600
44 0.3700 0.4300
45 0.1000 0.0875
46 0.1000 0.0875

[atom_types]
TC17 1039.88 24.25 0.00 0.00 735.31 17.15 12.01
CPC2 944.52 22.03 0.00 0.00 667.88 15.58 12.01
TC11 1802.24 34.18 0.00 0.00 1274.38 24.17 12.01
TH20 84.57 5.41 0.00 0.00 59.80 3.83 1.01
CPH18 0.00 0.00 0.00 0.00 0.00 0.00 1.01
CPC17 1103.59 24.67 0.00 0.00 780.35 17.44 12.01
CPN10 971.75 28.31 0.00 0.00 687.13 20.02 14.01
TC14 1039.88 24.25 0.00 0.00 735.31 17.15 12.01
TN13 971.75 28.31 70.50 1.581 687.13 20.02 14.01
TO12 616.44 23.77 0.00 0.00 435.89 16.81 16.00
HC1 84.57 5.41 0.00 0.00 59.80 3.83 1.01
TH21 84.57 5.41 0.00 0.00 59.80 3.83 1.01
TC7 944.52 22.03 0.00 0.00 667.88 15.58 12.01
CPO6 690.37 23.86 0.00 0.00 488.17 16.87 16.00
TN15 971.75 28.31 0.00 0.00 687.13 20.02 14.01
CPH27 0.00 0.00 0.00 0.00 0.00 0.00 1.01
TO4 445.13 18.25 0.00 0.00 314.75 12.91 16.00
H 0.00 0.00 0.00 0.00 0.00 0.00 1.01
CPH23 0.00 0.00 0.00 0.00 0.00 0.00 1.01
CPC3 944.52 22.03 0.00 0.00 667.88 15.58 12.01
CPC11 1802.24 34.18 0.00 0.00 1274.38 24.17 12.01
CPH22 84.57 5.41 0.00 0.00 59.80 3.83 1.01
TC16 1039.88 24.25 0.00 0.00 735.31 17.15 12.01
TO8 690.37 23.86 0.00 0.00 488.17 16.87 16.00
TH22 84.57 5.41 0.00 0.00 59.80 3.83 1.01
CPC5 944.52 22.03 0.00 0.00 667.88 15.58 12.01
TH23 0.00 0.00 0.00 0.00 0.00 0.00 1.01
TO1 760.65 25.04 0.00 0.00 537.86 17.71 16.00
CPH31 0.00 0.00 6.50 1.581 0.00 0.00 1.01
O2 616.44 23.77 70.00 1.581 435.89 16.81 16.00
HO 0.00 0.00 6.50 1.581 0.00 0.00 1.01
CPH30 109.18 6.99 0.00 0.00 77.20 4.94 1.01
CPO4 445.13 18.25 0.00 0.00 314.75 12.91 16.00
CPO8 690.37 23.86 0.00 0.00 488.17 16.87 16.00
TO6 690.37 23.86 0.00 0.00 488.17 16.87 16.00
CPH25 0.00 0.00 0.00 0.00 0.00 0.00 1.01
CPC14 1059.13 23.67 0.00 0.00 748.92 16.74 12.01
TH24 84.57 5.41 0.00 0.00 59.80 3.83 1.01
TN10 971.75 28.31 0.00 0.00 687.13 20.02 14.01
ODE 601.15 22.27 70.00 1.581 425.08 15.74 16.00
CPH24 84.57 5.41 0.00 0.00 59.80 3.83 1.01
C 1802.24 34.18 0.00 0.00 1274.38 24.17 12.01
CPC9 1039.88 24.25 0.00 0.00 735.31 17.15 12.01
CT 944.52 22.03 0.00 0.00 667.88 15.58 12.01
N 971.75 28.31 0.00 0.00 687.13 20.02 14.01
CPH28 0.00 0.00 0.00 0.00 0.00 0.00 1.01
HC 84.57 5.41 0.00 0.00 59.80 3.83 1.01
TH18 0.00 0.00 0.00 0.00 0.00 0.00 1.01
TH28 0.00 0.00 0.00 0.00 0.00 0.00 1.01
CPO1 760.65 25.04 0.00 0.00 537.86 17.71 16.00
TH19 84.57 5.41 0.00 0.00 59.80 3.83 1.01
TC5 944.52 22.03 0.00 0.00 667.88 15.58 12.01
CPH29 109.18 6.99 0.00 0.00 77.20 4.94 1.01
CPH19 84.57 5.41 0.00 0.00 59.80 3.83 1.01
CPO12 616.44 23.77 0.00 0.00 435.89 16.81 16.00
CPC16 1103.59 24.67 0.00 0.00 780.35 17.44 12.01
CPN13 971.75 28.31 70.50 1.581 687.13 20.02 14.01
TC9 1039.88 24.25 0.00 0.00 735.31 17.15 12.01
TH27 0.00 0.00 0.00 0.00 0.00 0.00 1.01
TC3 944.52 22.03 0.00 0.00 667.88 15.58 12.01
O 616.44 23.77 0.00 0.00 435.89 16.81 16.00
CPH20 84.57 5.41 0.00 0.00 59.80 3.83 1.01
CPN15 971.75 28.31 0.00 0.00 687.13 20.02 14.01
TH26 109.18 6.99 0.00 0.00 77.20 4.94 1.01

```
CPH21  84.57     5.41      0.00      0.00      59.80     3.83     1.01
C2    1802.24   34.18     0.00      0.00      1274.38   24.17    12.01
TH29  109.18    6.99      0.00      0.00      77.20     4.94     1.01
TC2   944.52    22.03     0.00      0.00      667.88    15.58    12.01
CPH26  109.18    6.99      0.00      0.00      77.20     4.94     1.01
CPC7  944.52    22.03     0.00      0.00      667.88    15.58    12.01
TH25  0.00      0.00      0.00      0.00      0.00      0.00     1.01
TH30  109.18    6.99      0.00      0.00      77.20     4.94     1.01

[change_atoms]
1  N  N
2  H  H
3  CT  CT
4  HC  HC
5  CT  CT
6  HC  HC1
7  HC  HC1
8  CT  CT
9  HC  HC
10  HC  HC
11  C2  C2
12  ODE  O2
13  O  O2
14  HO  CPH31
15  C  C
16  O  O
17  TO1  CPO1
18  TC2  CPC2
19  TC3  CPC3
20  TO4  CPO4
21  TC5  CPC5
22  TO6  CPO6
23  TC7  CPC7
24  TO8  CPO8
25  TC9  CPC9
26  TN10  CPN10
27  TC11  CPC11
28  TO12  CPO12
29  TN13  CPN13
30  TC14  CPC14
31  TN15  CPN15
32  TC16  CPC16
33  TC17  CPC17
34  TH18  CPH18
35  TH19  CPH19
36  TH20  CPH20
37  TH21  CPH21
38  TH22  CPH22
39  TH23  CPH23
40  TH24  CPH24
41  TH25  CPH25
42  TH26  CPH26
43  TH27  CPH27
44  TH28  CPH28
45  TH29  CPH29
46  TH30  CPH30

[soft_pairs]
12   14
14   29

[bond_types]
1 106.750  2.00  1.381
2 142.500  2.00  1.229
3 112.500  2.00  1.364
4 108.500  2.00  1.010
5 164.000  2.00  1.250
6 104.500  2.00  1.388
7 138.250  2.00  0.945
8 120.750  2.00  1.339
9 114.250  2.00  1.358
```

```
[change_bonds]
1538  1539  3    5
1538  1540  2    5
4427  4429  9    6
4429  4430  8    1
1539  1541  7    0
4429  1541  0    4

[angle_types]
1  70.000  116.800
2  70.000  113.000
3 140.000  117.000
4 160.000  120.400
5  70.000  118.000

[change_angles]
1535  1538  1540    4    3
1538  1539  1541    2    0
4427  4429  1541    0    1
4430  4429  1541    0    5

[torsion_types]
1   3.625   -2.000  180.000
2   2.450   -2.000  180.000
3   0.000   -1.000    0.000
4   1.500   -1.000    0.000
5   0.000    2.000  180.000
6   2.325   -2.000  180.000
7   0.000    3.000    0.000
8   0.000    1.000    0.000
9   2.450    2.000  180.000

[change_torsions]
1536  1535  1538  1540    5    0
1537  1535  1538  1540    5    0
1535  1538  1539  1541    4    0
1535  1538  1539  1541    9    0
1540  1538  1539  1541    9    0
1536  1535  1538  1540    0    8
1537  1535  1538  1540    0    8
4426  4427  4429  1541    0    3
4426  4427  4429  1541    0    6
4426  4427  4429  1541    0    7
4428  4427  4429  1541    0    3
4428  4427  4429  1541    0    2
4428  4427  4429  1541    0    7
1541  4429  4430  4431    0    3
1541  4429  4430  4431    0    1
1541  4429  4430  4431    0    7
1541  4429  4430  4432    0    3
1541  4429  4430  4432    0    1
1541  4429  4430  4432    0    7

[improper_types]
1     1.000   180.000

[change_impropers]
4427  4429  1541  4430    0    1

[off_diagonals]
1    2     12    29    1.00    0.50
```

C: Nucleophilic attack on the protonated cytidine

```
[atoms]
1  4416
2  4417
3  4418
4  4419
5  4420
6  4421
7  4422
8  4423
```

```
9  4424
10  4425
11  4426
12  4427
13  4428
14  4429
15  4430
16  4431
17  4432
18  4433
19  4434
20  4435
21  4436
22  4437
23  4438
24  4439
25  4440
26  4441
27  4442
28  4443
29  4444
30  4445
31  4446
32  4447
33  4448

[change_charges]
1  -0.6830  -0.6830
2  0.1450  0.1450
3  0.1700  0.1700
4  -0.4000  -0.4225
5  0.2050  0.2050
6  -0.7000  -0.7000
7  0.2050  0.2050
8  -0.7000  -0.7000
9  0.2225  0.5325
10  -0.2450  -0.6200
11  0.5000  0.6500
12  -0.5000  -0.3000
13  -0.5000  -0.7400
14  0.6450  0.6600
15  -0.9000  -0.8100
16  -0.1150  -0.0075
17  0.0075  0.1525
18  0.4180  0.4180
19  0.0600  0.0600
20  0.0600  0.0600
21  0.0300  0.0300
22  0.0600  0.0600
23  0.4350  0.4350
24  0.0600  0.0600
25  0.4350  0.4350
26  0.1000  0.1600
27  0.3600  0.4600
28  0.3600  0.4300
29  0.1150  0.0875
30  0.1150  0.0875
31  -0.6830  -1.200
32  0.4180  0.200
33  0.3000  0.4800

 [atom_types]
OHO1  856.00    0.00     70.00     1.581     856.00    23.01    16.00
CPC2  944.52    22.03     0.00     0.00     667.88    15.58    12.01
MO6   690.37    23.86     0.00     0.00     488.17    16.87    16.00
MC5   944.52    22.03     0.00     0.00     667.88    15.58    12.01
CPH18  0.00     0.00     0.00     0.00     0.00     0.00     1.01
MN15  1064.97   29.63     0.00     0.00     753.05    20.95    14.01
CPC17  1103.59   24.67     0.00     0.00     780.35    17.44    12.01
CPN10  971.75    28.31     0.00     0.00     687.13    20.02    14.01
MH19  84.57     5.41     0.00     0.00     59.80     3.83     1.01
CPO6  690.37    23.86     0.00     0.00     488.17    16.87    16.00
```

CPH27 0.00 0.00 0.00 0.00 0.00 0.00 1.01
CPH23 0.00 0.00 0.00 0.00 0.00 0.00 1.01
CPC3 944.52 22.03 0.00 0.00 667.88 15.58 12.01
CPC11 1802.24 34.18 0.00 0.00 1274.38 24.17 12.01
CPH22 84.57 5.41 0.00 0.00 59.80 3.83 1.01
MC3 944.52 22.03 0.00 0.00 667.88 15.58 12.01
MH25 0.00 0.00 0.00 0.00 0.00 0.00 1.01
CPC5 944.52 22.03 0.00 0.00 667.88 15.58 12.01
CPH31 0.00 0.00 0.00 0.00 0.00 0.00 1.01
MH23 0.00 0.00 0.00 0.00 0.00 0.00 1.01
MH18 0.00 0.00 0.00 0.00 0.00 0.00 1.01
MC7 944.52 22.03 0.00 0.00 667.88 15.58 12.01
CPH30 109.18 6.99 0.00 0.00 77.20 4.94 1.01
CPO4 445.13 18.25 0.00 0.00 314.75 12.91 16.00
MC11 1802.24 34.18 0.00 0.00 1274.38 24.17 12.01
CPO8 690.37 23.86 0.00 0.00 488.17 16.87 16.00
CPH25 0.00 0.00 0.00 0.00 0.00 0.00 1.01
CPC14 1059.13 23.67 71.00 1.581 748.92 16.74 12.01
MO31 760.65 25.04 70.00 1.581 537.86 17.71 16.00
MC9 944.52 22.03 0.00 0.00 667.88 15.58 12.01
CPH24 84.57 5.41 0.00 0.00 59.80 3.83 1.01
CPC9 1039.88 24.25 0.00 0.00 735.31 17.15 12.01
MO4 445.13 18.25 0.00 0.00 314.75 12.91 16.00
MH32 0.00 0.00 0.00 0.00 0.00 0.00 1.01
OHH2 0.00 0.00 0.00 0.00 0.00 0.00 1.01
CPH28 0.00 0.00 0.00 0.00 0.00 0.00 1.01
MO12 616.44 23.77 0.00 0.00 435.89 16.81 16.00
CPO1 760.65 25.04 0.00 0.00 537.86 17.71 16.00
MH28 0.00 0.00 0.00 0.00 0.00 0.00 1.01
CPH29 109.18 6.99 0.00 0.00 77.20 4.94 1.01
MN10 971.75 28.31 0.00 0.00 687.13 20.02 14.01
MO8 690.37 23.86 0.00 0.00 488.17 16.87 16.00
CPH19 84.57 5.41 0.00 0.00 59.80 3.83 1.01
MO1 760.65 25.04 0.00 0.00 537.86 17.71 16.00
CPO12 616.44 23.77 0.00 0.00 435.89 16.81 16.00
CPC16 1103.59 24.67 0.00 0.00 780.35 17.44 12.01
CPN13 971.75 28.31 0.00 0.00 687.13 20.02 14.01
MH22 84.57 5.41 0.00 0.00 59.80 3.83 1.01
MH20 84.57 5.41 0.00 0.00 59.80 3.83 1.01
MH26 84.57 5.41 0.00 0.00 59.80 3.83 1.01
MC17 1103.59 24.67 0.00 0.00 780.35 17.44 12.01
MC2 944.52 22.03 0.00 0.00 667.88 15.58 12.01
MH24 84.57 5.41 0.00 0.00 59.80 3.83 1.01
MC16 1103.59 24.67 0.00 0.00 780.35 17.44 12.01
MC14 944.52 22.03 71.00 1.581 667.88 15.58 12.01
CPH20 84.57 5.41 0.00 0.00 59.80 3.83 1.01
CPN15 971.75 28.31 0.00 0.00 687.13 20.02 14.01
MH33 0.00 0.00 0.00 0.00 0.00 0.00 1.01
MH27 0.00 0.00 0.00 0.00 0.00 0.00 1.01
MH30 69.58 4.91 0.00 0.00 49.20 3.47 1.01
CPH21 84.57 5.41 0.00 0.00 59.80 3.83 1.01
MH21 84.57 5.41 0.00 0.00 59.80 3.83 1.01
MH29 84.57 5.41 0.00 0.00 59.80 3.83 1.01
CPC7 944.52 22.03 0.00 0.00 667.88 15.58 12.01
CPH26 109.18 6.99 0.00 0.00 77.20 4.94 1.01
MN13 971.75 28.31 0.00 0.00 687.13 20.02 14.01

[change_atoms]
1 MO1 CPO1
2 MC2 CPC2
3 MC3 CPC3
4 MO4 CPO4
5 MC5 CPC5
6 MO6 CPO6
7 MC7 CPC7
8 MO8 CPO8
9 MC9 CPC9
10 MN10 CPN10
11 MC11 CPC11
12 MO12 CPO12
13 MN13 CPN13
14 MC14 CPC14

15 MN15 CPN15
16 MC16 CPC16
17 MC17 CPC17
18 MH18 CPH18
19 MH19 CPH19
20 MH20 CPH20
21 MH21 CPH21
22 MH22 CPH22
23 MH23 CPH23
24 MH24 CPH24
25 MH25 CPH25
26 MH26 CPH26
27 MH27 CPH27
28 MH28 CPH28
29 MH29 CPH29
30 MH30 CPH30
31 MO31 OHO1
32 MH32 OHH2
33 MH33 CPH31

[soft_pairs]
14 31

[bond_types]
1 106.750 2.00 1.381
2 80.000 2.00 1.410
3 120.250 2.00 1.340
4 112.000 2.00 1.365
5 84.250 2.00 1.449
6 122.500 2.00 1.335
7 79.250 2.00 1.510
8 104.500 2.00 1.388
9 84.250 2.00 1.463
10 106.750 2.00 1.433

[change_bonds]
4425 4426 6 8
4425 4432 1 4
4426 4428 6 8
4428 4429 5 1
4429 4430 9 3
4429 4431 7 10
4429 4446 2 0

[angle_types]
1 112.400 109.470
2 140.000 120.100
3 140.000 125.200
4 140.000 121.500
5 76.000 118.400
6 100.000 109.500
7 70.000 118.000
8 140.000 117.600
9 140.000 121.200
10 100.000 118.000
11 140.000 124.000
12 110.000 108.500
13 170.000 117.000
14 140.000 121.600
15 100.000 121.900
16 160.000 109.700

[change_angles]
4424 4425 4426 15 8
4424 4425 4432 10 9
4426 4425 4432 15 14
4426 4428 4429 15 3
4429 4428 4448 5 7
4428 4429 4431 16 4
4430 4429 4431 1 2
4429 4431 4432 11 13
4428 4429 4446 6 0

```
4430  4429  4446    6    0
4431  4429  4446    6    0
4429  4446  4447   12    0

[torsion_types]
1   0.234    3.000    0.000
2  -0.750   -1.000    0.000
3   0.250   -1.000    0.000
4   0.000   -2.000  180.000
5  -0.450   -1.000    0.000
6   0.000   -1.000    0.000
7   2.450   -2.000  180.000
8   0.000    3.000    0.000
9  -0.750   -2.000  180.000

[change_torsions]
4426  4428  4429  4446    2    0
4426  4428  4429  4446    9    0
4426  4428  4429  4446    8    0
4448  4428  4429  4446    6    0
4448  4428  4429  4446    7    0
4448  4428  4429  4446    8    0
4446  4429  4430  4442    6    0
4446  4429  4430  4442    7    0
4446  4429  4430  4442    8    0
4446  4429  4430  4443    6    0
4446  4429  4430  4443    7    0
4446  4429  4430  4443    8    0
4446  4429  4431  4432    3    0
4446  4429  4431  4432    4    0
4446  4429  4431  4432    8    0
4446  4429  4431  4445    6    0
4446  4429  4431  4445    4    0
4446  4429  4431  4445    1    0
4428  4429  4446  4447    6    0
4428  4429  4446  4447    4    0
4428  4429  4446  4447    8    0
4430  4429  4446  4447    6    0
4430  4429  4446  4447    4    0
4430  4429  4446  4447    8    0
4431  4429  4446  4447    5    0
4431  4429  4446  4447    4    0
4431  4429  4446  4447    8    0

[improper_types]
1    10.500   180.000
2     1.000   180.000

[change_impropers]
4448  4428  4426  4429    2    0
4426  4428  4448  4429    0    2
4430  4429  4431  4428    0    1
4443  4430  4429  4442    0    2

[off_diagonals]
1   2    14    31     1.00    0.50
```

D:

```
[atoms]
1  4416
2  4417
3  4418
4  4419
5  4420
6  4421
7  4422
8  4423
9  4424
10  4425
11  4426
12  4427
13  4428
14  4429
```

15 4430
16 4431
17 4432
18 4433
19 4434
20 4435
21 4436
22 4437
23 4438
24 4439
25 4440
26 4441
27 4442
28 4443
29 4444
30 4445
31 4446
32 4447
33 4448

[change_charges]
1 -0.6830 -0.6830
2 0.1450 0.1450
3 0.1700 0.1700
4 -0.4225 -0.4225
5 0.2050 0.2050
6 -0.7000 -0.7000
7 0.2050 0.2050
8 -0.7000 -0.7000
9 0.4725 0.5325
10 -0.5600 -0.6200
11 0.5500 0.6500
12 -0.4800 -0.3000
13 -0.5400 -0.7400
14 0.4600 0.6600
15 -0.7900 -0.8100
16 -0.0600 -0.0075
17 0.1000 0.1525
18 0.4180 0.4180
19 0.0600 0.0600
20 0.0600 0.0600
21 0.0300 0.0300
22 0.0600 0.0600
23 0.4350 0.4350
24 0.0600 0.0600
25 0.4350 0.4350
26 0.1300 0.1600
27 0.3700 0.4600
28 0.3700 0.4300
29 0.1000 0.0875
30 0.1000 0.0875
31 -0.8340 -1.200
32 0.4170 0.200
33 0.4170 0.4800

[atom_types]
TC17 1039.88 24.25 0.00 0.00 735.31 17.15 12.01
OHO1 856.00 0.00 70.00 1.581 856.00 23.01 16.00
CPC2 944.52 22.03 0.00 0.00 667.88 15.58 12.01
TC11 1802.24 34.18 0.00 0.00 1274.38 24.17 12.01
TH20 84.57 5.41 0.00 0.00 59.80 3.83 1.01
CPH18 0.00 0.00 0.00 0.00 0.00 0.00 1.01
CPC17 1103.59 24.67 0.00 0.00 780.35 17.44 12.01
CPN10 971.75 28.31 0.00 0.00 687.13 20.02 14.01
TO12 616.44 23.77 0.00 0.00 435.89 16.81 16.00
TN13 971.75 28.31 70.50 1.581 687.13 20.02 14.01
TC14 1039.88 24.25 0.00 0.00 735.31 17.15 12.01
TH21 84.57 5.41 0.00 0.00 59.80 3.83 1.01
TC7 944.52 22.03 0.00 0.00 667.88 15.58 12.01
CPO6 690.37 23.86 0.00 0.00 488.17 16.87 16.00
TN15 971.75 28.31 0.00 0.00 687.13 20.02 14.01
CPH27 0.00 0.00 0.00 0.00 0.00 0.00 1.01

```
TO4   445.13    18.25     0.00      0.00      314.75    12.91    16.00
CPH23  0.00      0.00      0.00      0.00      0.00      0.00     1.01
CPC3  944.52    22.03     0.00      0.00      667.88    15.58    12.01
CPC11  1802.24   34.18     0.00      0.00      1274.38   24.17    12.01
CPH22  84.57     5.41      0.00      0.00      59.80     3.83     1.01
TC16  1039.88   24.25     0.00      0.00      735.31    17.15    12.01
TO8   690.37    23.86     0.00      0.00      488.17    16.87    16.00
TH22  84.57     5.41      0.00      0.00      59.80     3.83     1.01
CPC5  944.52    22.03     0.00      0.00      667.88    15.58    12.01
TO1   760.65    25.04     0.00      0.00      537.86    17.71    16.00
TH23  0.00      0.00      0.00      0.00      0.00      0.00     1.01
CPH31  0.00      0.00      6.50      1.581     0.00      0.00     1.01
CPH30  109.18    6.99      0.00      0.00      77.20     4.94     1.01
CPO4  445.13    18.25     0.00      0.00      314.75    12.91    16.00
CPO8  690.37    23.86     0.00      0.00      488.17    16.87    16.00
TO6   690.37    23.86     0.00      0.00      488.17    16.87    16.00
CPH25  0.00      0.00      0.00      0.00      0.00      0.00     1.01
CPC14  1059.13   23.67     0.00      0.00      748.92    16.74    12.01
TH24  84.57     5.41      0.00      0.00      59.80     3.83     1.01
TN10  971.75    28.31     0.00      0.00      687.13    20.02    14.01
CPH24  84.57     5.41      0.00      0.00      59.80     3.83     1.01
CPC9  1039.88   24.25     0.00      0.00      735.31    17.15    12.01
OHH2  0.00      0.00      0.00      0.00      0.00      0.00     1.01
OW    762.89    24.39     70.00     1.581     539.45    17.25    16.00
CPH28  0.00      0.00      0.00      0.00      0.00      0.00     1.01
TH18  0.00      0.00      0.00      0.00      0.00      0.00     1.01
TH28  0.00      0.00      0.00      0.00      0.00      0.00     1.01
CPO1  760.65    25.04     0.00      0.00      537.86    17.71    16.00
TH19  84.57     5.41      0.00      0.00      59.80     3.83     1.01
TC5   944.52    22.03     0.00      0.00      667.88    15.58    12.01
CPH29  109.18    6.99      0.00      0.00      77.20     4.94     1.01
CPH19  84.57     5.41      0.00      0.00      59.80     3.83     1.01
CPO12  616.44    23.77     0.00      0.00      435.89    16.81    16.00
CPC16  1103.59   24.67     0.00      0.00      780.35    17.44    12.01
CPN13  971.75    28.31     70.50     1.581     687.13    20.02    14.01
HW    0.00      0.00      6.50      1.581     0.00      0.00     1.01
TH27  0.00      0.00      0.00      0.00      0.00      0.00     1.01
TC9   1039.88   24.25     0.00      0.00      735.31    17.15    12.01
TC3   944.52    22.03     0.00      0.00      667.88    15.58    12.01
CPH20  84.57     5.41      0.00      0.00      59.80     3.83     1.01
CPN15  971.75    28.31     0.00      0.00      687.13    20.02    14.01
TH26  109.18    6.99      0.00      0.00      77.20     4.94     1.01
CPH21  84.57     5.41      0.00      0.00      59.80     3.83     1.01
TH29  109.18    6.99      0.00      0.00      77.20     4.94     1.01
TC2   944.52    22.03     0.00      0.00      667.88    15.58    12.01
CPC7  944.52    22.03     0.00      0.00      667.88    15.58    12.01
CPH26  109.18    6.99      0.00      0.00      77.20     4.94     1.01
TH25  0.00      0.00      0.00      0.00      0.00      0.00     1.01
TH30  109.18    6.99      0.00      0.00      77.20     4.94     1.01

[change_atoms]
1  TO1  CPO1
2  TC2  CPC2
3  TC3  CPC3
4  TO4  CPO4
5  TC5  CPC5
6  TO6  CPO6
7  TC7  CPC7
8  TO8  CPO8
9  TC9  CPC9
10  TN10  CPN10
11  TC11  CPC11
12  TO12  CPO12
13  TN13  CPN13
14  TC14  CPC14
15  TN15  CPN15
16  TC16  CPC16
17  TC17  CPC17
18  TH18  CPH18
19  TH19  CPH19
20  TH20  CPH20
21  TH21  CPH21
```

```
22  TH22  CPH22
23  TH23  CPH23
24  TH24  CPH24
25  TH25  CPH25
26  TH26  CPH26
27  TH27  CPH27
28  TH28  CPH28
29  TH29  CPH29
30  TH30  CPH30
31  OW  OHO1
32  HW  OHH2
33  HW  CPH31

[soft_pairs]
13      33
31      33

[bond_types]
1 106.750  2.00  1.381
2 104.500  2.00  1.388
3 120.750  2.00  1.339
4 138.250  2.00  0.957
5 114.250  2.00  1.358
6 108.500  2.00  1.010

[change_bonds]
4426  4428  5    2
4428  4429  3    1
4446  4448  4    0
4428  4448  0    6

[angle_types]
1  70.000  116.800
2 200.000  104.520
3  70.000  118.000

[change_angles]
4447  4446  4448    2    0
4426  4428  4448    0    1
4429  4428  4448    0    3

[torsion_types]
1   0.000    3.000    0.000
2   2.325   -2.000  180.000
3   3.625   -2.000  180.000
4   2.450   -2.000  180.000
5   0.000   -1.000    0.000

[change_torsions]
4425  4426  4428  4448    0    5
4425  4426  4428  4448    0    2
4425  4426  4428  4448    0    1
4427  4426  4428  4448    0    5
4427  4426  4428  4448    0    4
4427  4426  4428  4448    0    1
4448  4428  4429  4430    0    5
4448  4428  4429  4430    0    3
4448  4428  4429  4430    0    1
4448  4428  4429  4431    0    5
4448  4428  4429  4431    0    3
4448  4428  4429  4431    0    1

[improper_types]
1     1.000   180.000

[change_impropers]
4426  4428  4448  4429    0    1
[off_diagonals]
1   2    31    33     1.00    0.50
```

Acknowledgments

I would like to thank my supervisor Johan Åqvist because of this opportunity to work on this topic and all his helps during this period. I also would like to thank Assistant Prof. Shina Lynn Kamerlin and Henrik Keränen because of all their helps and friendship.

References

1 Breneman C M and Wiberg K B. 1990. Determining atom-centered monopoles from molecular electrostatic potentials - the need for high sampling density in formamide conformational-analysis. Journal of Computational Chemistry. 11:361-73.

2 Carlow D C, Short S A, Wolfenden R. 1998. Complementary truncations of a hydrogen bond to ribose involved in transition-state stabilization by cytidine deaminase. Biochemistry 37:1199-203.

3 Carlow D C, Smith A A, Yang C C, Short S A, Wolfenden R. 1995. Major contribution of a carboxymethyl group to transition-state stabilization by cytidine deaminase: mutation and rescue. Biochemistry 34:4220-4.

4 Cossi M, Rega N, Scalmani G, and Barone V. 2003. Energies, structures, and electronic properties of molecules in solution with the C-PCM solvation model. Journal of Computational Chemistry. 24:669-81.

5 Frick L, Macneela JP, Wolfenden R. 1987. Transition state stabilization by deaminases: Rates of nonenzymatic hydrolysis of adenosine and cytidine. Bioorganic Chemistry. 15: 100-108.

6 Frisch M J, Trucks G W, Schlegel H B, Scuseria G E, Robb M A, Cheeseman J R, Scalmani G, Barone V, Mennucci B, Petersson G A, Nakatsuji H, Caricato M, Li X, Hratchian H P, Izmaylov A F, Bloino J, Zheng G, Sonnenberg J L, Hada M, Ehara M, Toyota K, Fukuda R, Hasegawa J, Ishida M, Nakajima T, Honda Y, Kitao O, Nakai H, Vreven T, Montgomery Jr J A, Peralta J E, Ogliaro F, Bearpark M, Heyd J J, Brothers E, Kudin K N, Staroverov V N, Kobayashi R, Normand J, Raghavachari K, Rendell A, Burant J C, Iyengar S S, Tomasi J, Cossi M, Rega N, Millam N J, Klene M, Knox J E, Cross J B, Bakken V, Adamo C, Jaramillo J, Gomperts R, Stratmann R E, Yazyev O, Austin A J, Cammi R, Pomelli C, Ochterski J W, Martin R L, Morokuma K, Zakrzewski V G, Voth G A, Salvador P, Dannenberg J J, Dapprich S, Daniels A D, Farkas Ö, Foresman J B, Ortiz J V, Cioslowski J, Fox D J, Gaussian, Inc. Wallingford CT, 2009.

7 Josefredo R. Pliego Jr. 2003. Thermodynamic cycles and the calculation of pKa. Chemical Physics Letters. 367:145–149

8 Josefredo R, Pliego Jr and Riveros J M. 2002. Gibbs energy of solvation of organic ions in aqueous and dimethyl sulfoxide solutions. Physical Chemistry Chemical Physics. 4:1622-1627

9 Kamerlin S C, Haranczyk M, Warshel A. 2009. Progress in ab initio QM/MM free-energy simulations of electrostatic energies in proteins: accelerated QM/MM studies of pKa, redox reactions and solvation free energies. Journal of Physical Chemistry B. 113:1253-72.

10 Leach A R. 2001. Molecular Modeling Principles and applications. second edition. Pearson education.

11 Marelius J, Kolmodin K, Feierberg I, Aqvist J. 1998. Q: a molecular dynamics program for free energy calculations and empirical valence bond simulations in biomolecular systems. Journal of Molecular Graphics and Modeling. 16:213-25.

12 Marenich A V, Cramer J C, and Truhlar D G. 2009. Universal solvation model based on solute electron density and a continuum model of the solvent defined by the bulk dielectric constant and atomic surface tensions. Journal of Physical Chemistry. 13:6378-96.

13 Snider M J, Gaunitz S, Ridgway C, Short S A, Wolfenden R. 2000. Temperature effects on the catalytic efficiency, rate enhancement, and transition state affinity of cytidine deaminase, and the thermodynamic consequences for catalysis of removing a substrate "anchor". Biochemistry 39:9746-

53.

14 Snider M J, Reinhardt L, Wolfenden R, Cleland W W. 2002. 15N kinetic isotope effects on uncatalyzed and enzymatic deamination of cytidine. Biochemistry 41:415-21.

15 Warshel A. 1991. Computer Modeling of Chemical reactions in enzymes and solutions. A wiley interscience publication. John Wiley and Sons INC.

16 Xiang S, Short S A, Wolfenden R, Carter C W Jr. 1995. Transition-state selectivity for a single hydroxyl group during catalysis by cytidine deaminase. Biochemistry 34 :4516-23.

17 Xiang S, Short S A, Wolfenden R, Carter C W Jr. 1996. Cytidine deaminase complexed to 3-deazacytidine: a "valence buffer" in zinc enzyme catalysis. Biochemistry 35:1335-41.

18 Xiang S, Short S A, Wolfenden R, Carter C W Jr. 1997. The structure of the cytidine deaminase-product complex provides evidence for efficient proton transfer and ground-state destabilization. Biochemistry 36:4768-74.